Acta Physica Universitatis Comenianae
Vol. LII (2011) 19 32

The Study of the Interaction of Cytochrome c with Calixarenes Incorporated into the Vesicles or Supporting Lipid Films

T. Hianik[1*], A. Poturnayová[2], M. Šnejdárková[2], Z. Garaiová[1], V. Vargová[1], I. Karpišová[1]

[1]Department of Nuclear Physics and Biophysics, Comenius University, Mlynská dolina F1, 842 48 Bratislava, Slovakia
[2]Institute of Animal Biochemistry and Genetics, Slovak Academy of Sciences, 900 28 Ivánka pri Dunaji, Slovakia

Abstract: We applied the dynamic light scattering method to measure the size and zeta potential of large unilamellar vesicles (LUV) composed of dimyristoylphosphatidylcholine (DMPC) and containing calix[6]arene (CX) specific to cytochrome c (cyt c). We also used quartz crystal microbalance (QCM) and atomic force microscopy (AFM) methods to study the interaction of cyt c with supporting lipid films (sBLM) of DMPC containing CX. The 10 mol % CX induced increase in average size of LUV by approx. 1.2 times. This has been accompanied by decrease of zeta potential to more negative values, which is connected with negatively charged carboxyl groups of polar part of CX. Cyt c caused partial neutralization of negative the zeta potential due to specific interaction with CX. QCM method indicated decrease of the resonant frequency connected with increase of the mass of cyt c at the surface of sBLM modified by CX. However, even at rather high concentration of cyt c (0.8 mM) the saturation in frequency changes was not observed. This suggests the formation of cyt c aggregates or fibers. This effect has been confirmed by AFM.

Keywords: Calixarenes, Cytochrome c, Supported lipid films, Large unilamellar vesicles, Dynamic light scattering, Quartz crystal microbalance, AFM

***Corresponding author:** *tibor.hianik@fmph.uniba.sk* (T. Hianik)

1. Introduction

The vesicles and supported bilayer lipid membranes (sBLM) are convenient models of biomembranes [1]. In particular, they serve for study of the mechanisms of interactions of proteins with the cell surface. In recent years the sBLMs have been extensively used also as a tool for construction biosensors [2]. The lipid films could be modified by proteins or synthetic receptors and serve as recognition devices for medical diagnosis. Among receptors the calixarenes are of increased interest due to their sensitivity and selectivity to low or high molecular weight ligands [3]. Calix[n]arenes are macrocyclic aromatic molecules, which originate from the synthesis of the phenols and aldehydes, whereas [n] refers to the number of the phenol aromatic cycles in the molecule. The phenol subunits are bridged via methyl groups. This provides the characteristic vase-like shape of the calixarene molecule. Due to the presence of the hydrophobic cavity, formed by the phenol units, calixarenes are

being used for detection of a wide range of compounds such as metal ions, nucleosides, amino acids or proteins [4]. Moreover, modification of the side groups of calixarenes allows one to prepare tailor-made receptors with a high affinity for specific target molecules. Recently the calixarene sensitive to cytochrome c (cyt c) has been synthesized [5]. Cyt c is small hemoprotein (molecular weight 12.4 kDa) found in the intermembrane space of mitochondria. At physiological conditions it is positively charged thanks to lysine and arginine amino acid residues. Cyt c plays dual role in a living system. Firstly it participates in electron transport and secondly, it is responsible for activation of the apoptotic pathway through releasing from mitochondria into the cytosol [6]. Many studies have been focused on interaction of cyt c with lipid membranes (see [7] and references herein). In particular, it has been shown that cyt c induced transition of lamellar phase composed of phosphatidylcholine and cardiolipin (CL) into the hexagonal phase which is favorable for transport of cyt c through hydrophobic part of the membrane [7]. The CL is an important component of mitochondria membranes. At the same time, the detection of endogenous concentration of cyt c is of a high importance for diagnosis of possible pathological processes in the organism. The selective extraction of cyt c with calix[6]arene carboxylic acid derivative (^{t}Oct[6]CH_2COOH) has been described by Oshima et al. [5]. This calixarene can therefore serve as a recognition element in sensor for detection cyt c. The principle of interaction of cyt c with calix[6]arene is based on sensitivity of the calixarene to the amino groups of lysine at the surface of the protein. Totally there are 19 lysine residues at the surface of cyt c available for interaction with calixarene. Lysine is the basic amino acid containing two amino groups: and . – amino group participates on peptide bound in cyt c, while amino group is free and positively charged at physiological conditions (pH 7). This amino group participates at formation of hydrogen bonds and interacts with the cavity of calix[6]arene. We have shown recently that this calixarene can form stable monolayers at an air-water interface and can be incorporated into the bilayer lipid membranes (BLM). Its presence in mixed monolayers and in BLM resulted in decrease of the compressibility in lateral direction and in direction perpendicular to the BLM plane, respectively [8]. sBLM containing this calixarenes has also been recently shown as an efficient sensor for detection cyt c [9]. However, in order to understand better the mechanisms of interaction cyt c with the calixarene incorporated in the lipid films, further studies are required using additional physical methods.

In this work we used the dynamic light scattering method for study of the size and zeta potential of large unilamellar vesicles (LUV) modified by calixarenes, quartz crystal microbalance (QCM) to analyze the interaction of cyt c with sBLM and atomic force microscopy (AFM) to study the topography of the surfaces of sBLM containing calixarenes.

2. Experimental

2.1. Chemicals

All chemicals were of the highest purity commercially available: 1,2-sn-glycero-dimyristoylphosphatidylcholine (DMPC) was purchased from Avanti Polar Lipids Inc. (USA), cyt c from bovine heart was supplied by Sigma-Aldrich (USA). Calix[6]arene carboxyl acid derivative (^{t}[6]CH_2COOH) (CX) was a generous gift by Dr. T. Oshima (University of Miyazaki, Japan) and synthesized according to the procedure described else-

where [10]. Phosphate buffered saline (PBS), pH 7.4, was prepared by dissolving the tablets (Sigma Aldrich) in a highly purified deionized water (ELIX 5, Millipore, USA) and used in all experiments.

2.2. Preparation of large unilamellar vesicles (LUV)

LUV were prepared by the extrusion method described in Ref. [11]. Briefly, either DMPC or its mixture with CX (1, 3, 10 mol%) dissolved in chloroform was added into the round glass flask and evaporated under a nitrogen stream. The dry lipid film was hydrated with PBS buffer with a continuous shaking. In all cases the final concentrations of the lipids were 4 mg/ml or 0.4 mg/ml for size and zeta potential measurements, respectively. This procedure yields multilamellar vesicles. The solutions were subsequently extruded through Milipore polycarbonate filters (100 nm pore size) using extruder (Avanti Polar Lipids) at a temperature 30 C, which was well above the main phase transition temperature of DMPC. In experiments the desired amount of cyt c stock solution in PBS was added into the vesicle suspension and incubated for 10 min. For preparation of sBLM in QCM experiments the LUV were prepared in PBS containing 3 mM $CaCl_2$.

2.3. Preparation of sBLMs

sBLMs for QCM experiments were prepared by the liposome fusion as described elsewhere [12]. Briefly, the 1-octadecanethiol (ODT) (Sigma-Aldrich) dissolved in chloroform in a concentration 10 mM has been added onto the clean gold surface of quartz crystal transducer of an area 0.2 cm^2 (CH Instruments, USA) and incubated during 12 h at 4 C (For the cleaning procedure see [13]). Then the surface was washed with chloroform, dried in a stream of nitrogen and mounted into the flow QCM cell. The surface of the cell was washed by PBS and subsequently LUV (2 mg/ml) without or with CX (10 mol%) has been allowed to flow in a rate 50 l/min using Genie Plus syringe pump (Kent Scientific, USA). As soon as the vesicles reached the crystal surface the flow has been stopped for 90 min. This time was sufficient for formation of lipid monolayer at the top of ODT [12]. The cell was then washed with PBS flow until the steady state frequency of the crystal was established. Then the cyt c in PBS has been added. After each addition of cyt c and establishing steady state value of resonant frequency the surface was washed with PBS to remove the weakly adsorbed protein.

sBLM for AFM experiments were prepared on a freshly cleaved mica surface (25 25 mm^2) (V2-grade, Pelco USA) as follows. The DMPC and CX were dissolved in chloroform in a concentration 2.5 mg/ml. For mixed DMPC membranes the 10 mol% of CX was used. The drop (approx. 10 l) of the pure or mixed component mentioned above has been added on the mica surface and allowed to dry in an air. The resulted film has been then hydrated in a PBS at temperature 32 C during at least 45 min. This temperature is well above the main phase transition of DMPC (24 C) and ensures the proper formation of the bilayer. Because freshly cleaved mica surface is hydrophilic, we assume that the zwitterionic phosphatidylcholine head groups of DMPC will contact with the surface and hydration in a buffer will result in formation of the lipid bilayers or multilayers. Prior the AFM measurements, the layer has been several times gently washed with a PBS. Similarly also pure calixarene layers were prepared. In addition to the images of pure self-assembled membranes (SAM) also that at presence of 30 nM of cyt c were analyzed. For this

purpose the drop (10 l) of cyt c in a buffer has been added onto the surface of SAM and incubated during 30 min. The surface has been then gently washed by a buffer.

2.4. Size and zeta potential measurements

Vesicle size and zeta potential measurements were made by the dynamic light scattering method using a Zetasizer Nano ZS (Malvern Instruments, UK) at 20 C or 28 C. The LUV in a concentration of 4 mg/ml or 0.4 mg/ml were used for the measurement of size or zeta potential, respectively.

2.5. QCM experiments

A QCM home made apparatus was based on SN74LS320 crystal-controlled oscillator (Texas Instruments, USA) and constructed according to Skladal and Horacek [14]. The oscillation frequency changes were measured by means of UZ 2400 frequency meter (Grundig, Germany) connected to IBM PC Pentium through a RS232 interface. The frequency was measured with accuracy of 1 Hz. For the preparation of the sBLM we used AT-cut quartz with a fundamental frequency of 8 MHz (CH Instrumnets, USA), covered on both sides by polished gold electrodes (working area 0.2 cm^2).

2.6. Atomic force microscopy

AFM scans were obtained by computer-controlled magnetic mode 5500 AFM Agilent Technologies (Tempe AZ, USA) in tapping mode using N9521A multipurpose scanner 90 m and MAC Levers, type II Si cantilever of 225 m length with a force constant 2.8 N/m and a typical tip curvature 10 nm. The resonance frequency of the cantilever in a buffer was around 40 kHz. The measurements were performed in a buffer at temperature 29 C. Usually 3–6 scans were performed at least for 3 independently prepared samples. Dimensions of the scans varied between 10 10 m^2 and 1 1 m^2. AFM images were performed in the topographical mode. The given Z-scale in all presented AFM images is relative, because we subtracted the second-order polynomial background to remove the large-scale differences from the scans. Obtained surface images and the root mean square roughness (R_{rms}) were analyzed by PicoScan software version 5.3.3. (Agilent Technologies) and Origin version 8.0 Microcal Software, Inc. (USA). The R_{rms} values were determined according to the following equation [15]:

$$R_{rms} \quad \sqrt{\frac{1}{N_x N_y} \sum_{i\ 1}^{N_x} \sum_{j\ 1}^{N_y} (z(i,j) \quad z_{mean})^2} \qquad (1)$$

where N_x, N_y are the dimensions of the image (number of data points in each coordinate); z depicts the surface height at the particular pixel position (i,j); and z_{mean} is the mean height.

3. Results and discussion

3.1. Size and zeta potential of LUV

In the first series of experiments, we analyzed the size and zeta potential of LUV from pure DMPC and that containing different concentrations of calixarenes (CX). We also studied the effect of cyt c on the properties of vesicles containing 10 mol% of CX. The average diameter and zeta potential of LUV as a function of molar concentration of CX are

shown in Fig. 1 A and B, respectively. The average diameter was studied at temperature below (20 C) and above (28 C) the main phase transition of DMPC from gel to liquid-crystalline state. The average diameter of pure DMPC in a gel state of the bilayers (T = 20 C) was 96.0 1.7 nm which agree well with the diameter of the pores of polycarbonate filter used in extrusion method (100 nm). Also the reproducibility of the measurement was rather high. The S.D. obtained from 3 independent experiments did not surpass 1.8 %. The average diameter of LUV in a liquid crystalline state (T = 28 C) was 105.1 1.3 nm. This is significantly higher in comparison with that in a gel state of DMPC bilayer according to the t-test ($p < 0.01$). This effect is connected mostly with increase of mean molecular area of phospholipids in a liquid crystalline state of the bilayer and agrees well with experiments on lipid monolayers [16]. With increased content of CX the average size also significantly increases both in gel and liquid crystalline state of DMPC bilayer (Fig. 1 A) according to t-test ($p < 0.01$). This phenomenon is due to increase of the mean molecular area of molecules composed of the bilayers and agrees well with our recent experiments on monolayers composed of diphytanoyl phosphatydilcholine (DPhPC) containing various molar concentrations of CX. The reason of this effect is in substantially larger mean molecular area of CX (3.3 ± 0.04 nm^2) in comparison with DPhPC (1.04 ± 0.02 nm^2) in its solid state. For example, the mean molecular area of DPhPC containing 10 mol% of CX was 1.4 ± 0.03 nm^2, i.e. increased by 1.35 times in comparison with that of pure DPhPC.

Zeta potential (potential) or electrokinetic potential is the electrostatic potential at shear plane of the particles. The determination of zeta potential allows estimation of the Gouy-Chapman potential, which is an informative value on charge density at the surface of lipid bilayer [17]. The plot of zeta potential as a function of CX molar concentration in DMPC LUV is presented in Fig. 1B. The zeta potential of pure DMPC is only slightly negative (–1.6 1.1 mV) which reflects the zwitterionic nature of DMPC polar head groups. It can be seen that with increased molar concentration of CX the zeta potential became more negative and, at 10 mol% of CX, it reached significantly lower value –20.8 0.7 mV in comparison with pure DMPC ($p < 0.01$ according to t-test). This behavior is expected and is due to negatively charged carboxyl groups at the polar part of the calixarenes. The

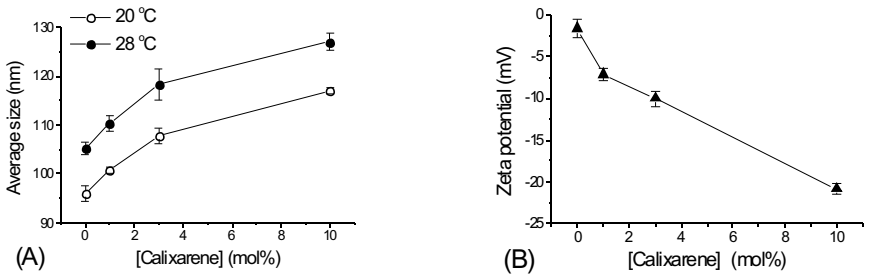

Fig. 1. The plot of the average size (A) and zeta potential (B) of LUV composed of DMPC as a function of molar content of calixarene. The average side was measured at temperatures below (20 C) and above (28 C) the main phase transition of DMPC, while zeta potential was measured at temperature 20 C. The results represent the mean ± S.D. obtained in 2–3 measurements in each series.

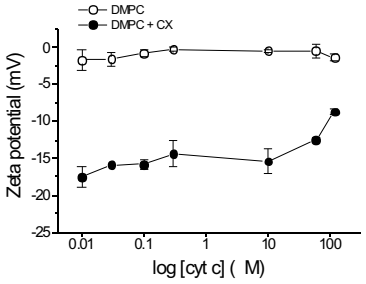

Fig. 2. The plot of zeta potential as a function of cyt c concentration for pure DMPC LUV and that containing 10 mol% of CX, see the legend.

changes of zeta potential with increased molar content of CX are also a convincing evidence of incorporation of the CX into the LUV. Due to relatively short hydrophobic butyl residues in CX molecule [5] we expect that CX is localized mostly at the LUV surface and not deeply incorporated into the lipid bilayer. This conclusion follows also from AFM experiments (see below).

We studied also the interaction of cyt c with pure DMPC LUV and that containing 10 mol% of CX in a gel state of lipid bilayers (T = 20 C). Cyt c in a concentration range of 0–118 M had practically no effect on the size of pure DMPC LUV and that containing CX (results are not shown). However, zeta potential of DMPC modified by CX changed significantly at concentration of cyt c above 10 M and became more positive. At the same time, practically no changes of this value were observed for pure DMPC (Fig. 2), which suggests that cyt c practically does not interact with the head group of zwitterionic phospholipids in a gel state. This agrees well with previous studies [18]. The more positive value of zeta potential at higher cyt c concentrations for LUV containing CX are due to compensation of negative charge of vesicles caused by incorporation of positively charged cyt c by its lysine amino group into the cavity of CX [5].

Thus, the results obtained clearly indicate that CX is incorporated into the LUV and it caused increase of the average size of vesicles. Moreover, cyt c caused compensation of negative charge of vesicles contained CX. In order to obtain more information about binding properties of cyt c to the CX containing lipid layer, we performed experiments using the QCM method.

3.2. The study of interaction of cyt c with sBLM using QCM method

The QCM is a highly efficient method for studying affinity interaction at surface. The theory of QCM is described in many reviews, see for example [14]. Briefly, for the rigid and ultrathin film the Sauerbrey equation (2) describes the relationship between the changes of resonant frequency (*f*) and the adsorbed mass (m) [19]:

$$f \quad 2f_0^2 \ _s(\ _q \ _q)^{1/2} \quad 2.26 \ \ 10^{-6} f_0^2 (\ m/A) \qquad (2)$$

(f_0 is the fundamental frequency of the quartz, $_S$ is the mass density, $_q$ 2.95 10^{10} Pa is the shear stiffness of quartz, $_q$ = 2650 kg m^{-3} is the quartz density and A is the active area). In Eq. (2) the surface mass loading (m/A) is in g.cm^{-2} [20]. This equation is valid for dry

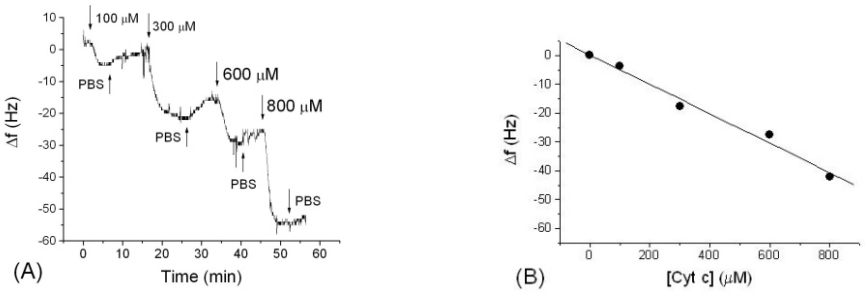

Fig. 3 A. The kinetics of the changes of resonant frequency following addition of the cyt c to a surface of biolayer composed of DMPC and CX (10 mol%) and washing the surface by PBS flow. Moment of starting flow is shown by arrows. **B.** The plot of resonant frequency changes as a function of cyt c concentration.

crystal in vacuum. The oscillations of quartz in a liquid are, however, affected by viscosity of surrounding liquid, which cause additional frequency changes [21]. However, for analytical purposes even Eq. (2) can be used assuming that a correction factor of approx. 2 could be applied to correct changes of frequency affected by viscoelasticity [22]. I.e., viscoelasticity causes approx. 2 times larger decrease of the frequency change in comparison with the mass effect only. However, exact correction of frequency changes has to be determined in special experiment using impedance analysis of crystal oscillations by means of vector network analyzer [23]. In the experiments, we measured the changes of frequency following various modification of the surface of crystal transducer. The addition of LUV modified by CX to a surface of the crystal with chemisorbed ODT layer resulted in substantial decrease of frequency by 118 0.5 Hz, which is a clear evidence of formation of a lipid monolayer. We did not observe significant frequency changes when cyt c was added to a surface of sBLM without CX (results are not shown). However, the addition of cyt c to a sBLM containing CX resulted in the decrease of resonant frequency. It is clearly seen from the kinetics of the changes of the resonant frequency (Fig. 3A). After each addition of the cyt c the surface of the biolayer has been washed by flow of the buffer. The increase of the frequency followed by the washing step is the evidence of desorption of weakly adsorbed protein. The plot of the frequency changes as a function of cyt c concentration is shown in Fig 3 B. It is interesting that even at relatively large concentration of cyt c no saturation has been observed. In fact, knowing the molecular area of phospholipids and CX, it is possible to estimate the number of CX molecules in a transducer surface and estimate the surface concentration of cyt c at which all CX binding sites are occupied by protein. Taking into account that the mean molecular area of DMPC is approx. 0.5 nm^2 [24] and that of CX is 3.3 nm^2 [8], the number of CX molecules at the transducer surface of the area 0.2 cm^2 is approx. 2 10^{11}. If only one molecule of cyt c binds to the calixarene, we could expect saturation already at nanomolar concentrations. However, as it is seen from the plot of the changes of frequency as a function of cyt c concentration (Fig. 3B), the resonant frequency continues to decrease almost linearly even at extremely large protein concentration. This is only possible when cyt c forms aggregates. We certainly confirmed the existence of this effect using the AFM method.

3.3. AFM images of sBLM containing calixarenes

The AFM scan of the DMPC layer and the thickness profile of the layer is shown in Fig. 4. The R_{rms} value of the layer was 0.29 nm, which means that DMPC forms rather flat layer containing islands of small aggregates (see upper part of the image). The height difference between mica surface and the upper part of DMPC layer was between 3 and 4 nm, which correspond to the lipid bilayer and agrees well with results published earlier [25]. The bilayer structure of DMPC is well discriminated in 3D image showed in Fig. 4C. However, the above conclusion should be confirmed in independent experiments using the phase contrast method. It is quite probable that in addition to lipid bilayers also the patches containing multilayers are present at the mica surface (see Fig. 8).

According to our knowledge the calixarene ^{t}Oct[6]CH_2COOH has not been characterized by AFM yet. Therefore we studied the topography of the layers of this calixarene on a mica surface in detail. For this purpose the calixarene layer has been formed similarly to that of DMPC. The drop (10 l) of the CX stock solution in a chloroform (2.5 mg/ml) has been added to the surface of freshly, cleaved mica and allowing drying at an air during 15 min at room temperature (approx. 22 C). The surface was then gently washed with a PBS. The AFM scans were performed in a PBS at the same conditions like those for DMPC. The resulting scan of the area 10 10 m^2, R_{rms} profile and 3D image of calixarene layer are presented in Fig. 5. The roughness of the surface (R_{rms} = 1.51 nm) was approx. 5 times larger in comparison with that of DMPC. Most dark parts correspond to the uncovered mica or CX monolayers, while more light part are the CX multilayers or their aggregates. From the profile of the image (Fig. 5B), it is possible to determine the height of particular structures, which is around 1.5–2 nm for dark regions, and around 9 nm for

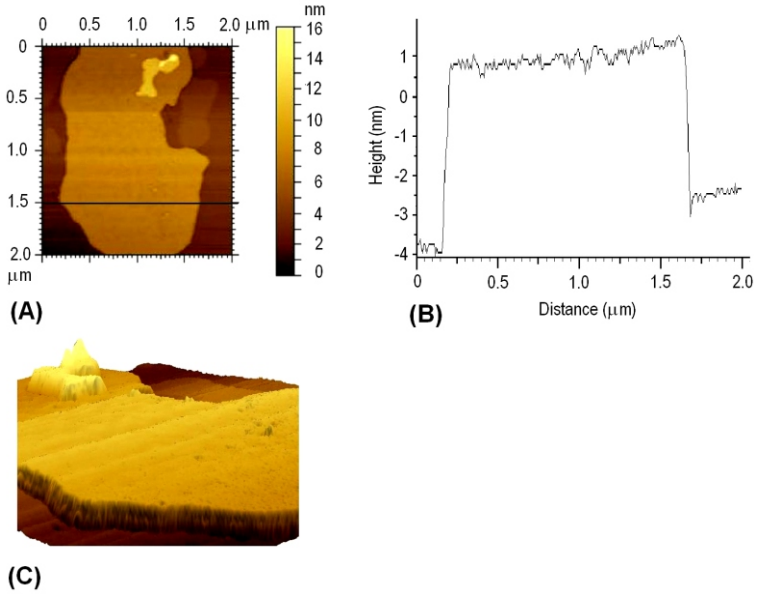

Fig. 4. AFM image of the DMPC layer at mica surface of the area 2 2 m^2: (A) 2D scan; (B) profile of the thickness along the line drawn in the image; (C) 3D image.

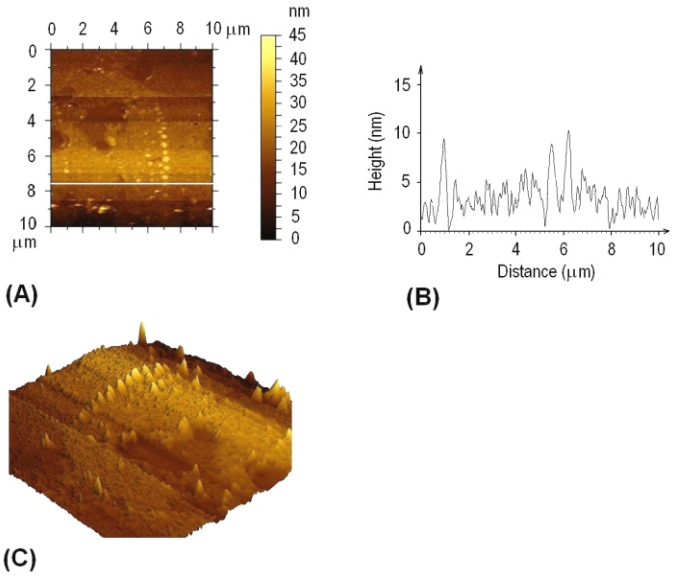

Fig. 5. AFM image of the CX layer at mica surface of the area 10 10 m^2: (A) 2D scan; (B) profile of the thickness along the line drawn in the image; (C) 3D image.

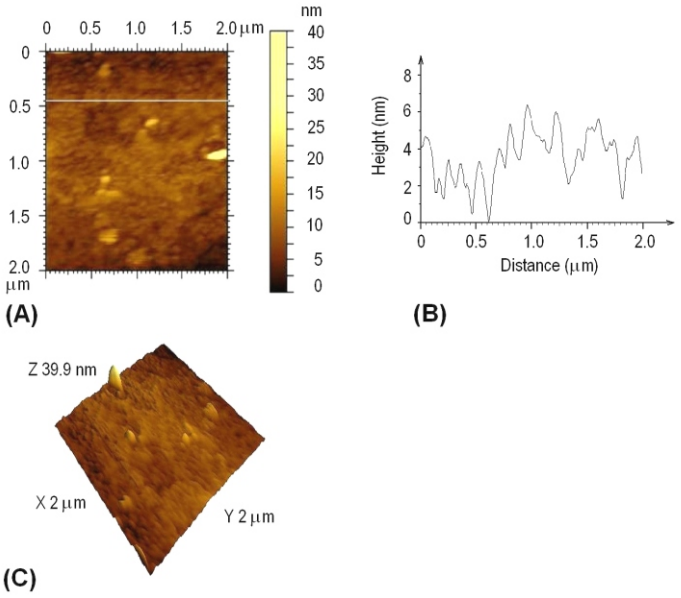

Fig. 6. AFM image of the ^{t}Oct[6]CH_2COOH layer at mica surface of the area 2 2 m^2: (A) 2D scan; (B) profile of the thickness along the line drawn in the image; (C) 3D image.

bright parts. The structure with height of 1.5– 2 nm probably corresponds to individually adsorbed CX molecules while the thicker structures are CX aggregates.

The image of scanned area 2 2 μm^2 allowing analyzing the surface of CX in more detail (Fig. 6A). We selected the area of the surface contained higher surface density of the CX monolayers. From the profile of the surface (Fig. 6B) it can bee seen that the roughness of this part is R_{rms} = 0.94 nm and that for all scanned surface is S_q = 2.74 nm which is also higher in comparison with that for pure DMPC layer. We should note that the CX molecule contains at one side the hydrophilic carboxylic acid residues, which probably contact with hydrophilic surface of the mica. The hydrophobic butyl chains at opposite side of phenol rings of CX could favorably interact with the same side of other CX molecule. Thus the self-assembled CX multilayers could be formed in a buffer. Taking into account that the dimension of the CX is around 2 nm from the profile showed on Fig. 6B we can expect formation at least 4 layers.

We studied also the mica surface covered by a layer composed of a mixture of DMPC and CX (10 mol % of CX). The roughness of the surface at the marked profile was rather large, R_{rms} = 19.4 nm, and the average surface roughness was S_q = 39.5 nm. The surface can be characterized by hole like defects. The holes are surrounded by structures of a spherical shape. It can be seen from the cross sectional profile of this scan that heights of these structures are in the interval of units to hundreds nm. It can be seen from 3D image (Fig. 7C) and from its zoom (Fig. 7D) that the rippled surface contains sharp structures and regularly repeated circular holes. The structures of cylindrical shapes are visible in a more detailed image of the smaller area 2 2 μm^2 (Fig. 8). These cylindrical structures alternate with the holes in the layer. However, it is difficult to see structures corresponding to the individual CX due to rather large fluctuations of cross-sectional profile and large thickness of the layer.

We studied also the topography of the mixed DMPC-CX layer at the mica surface following 40 min incubation with 30 nM of cyt c. Interestingly the topography of the layer changed substantially in comparison with that without cyt c. The roughness along the cross sectional line presented in Fig. 9A was much lower: R_{rms} = 1.1 nm and S_q = 0.95 nm in average for whole surface. It is likely that cyt c affect the structure of DMPC layer in a fluid state by desorption of lipid patches from the surface of the DMPC multilayer film. This agrees well with recently reported studies of interaction of cyt c with mixed DOPC/DPPC layers at mica surface [26]. However, in addition to the relatively flat surface, we observed also rather sharp peaks of a height up to 16 nm, which may be connected with adsorbed cyt c that form column like aggregates. This phenomenon has been already mentioned above in Section 3.2. At more detailed scan of the selected area of 1 1 m^2 the sharp peaks of cyt c of a height 7 nm are observed (Fig. 10). For this scan the surface roughness was S_q = 0.60 nm and that in a marked cross sectional line R_{rms} = 0.97 nm. This is still larger than the roughness of DMPC layer, but average roughness is only 2 times higher in comparison with that for pure DMPC layer. The sharp aggregates of cyt c were observed only at the presence of CX, but not for pure DMPC layers, which suggest specific interaction of cyt c with the layers containing CX. We did not observe changes in topography of DMPC layers without CX at the gel state of DMPC (T = 20 C). Interestingly, the formation of cyt c fibers on a surface of vesicle containing anionic lipid phosphatidylserine has been reported. AFM study confirmed the existence of the fibers of a diameter 3–4 nm [27].

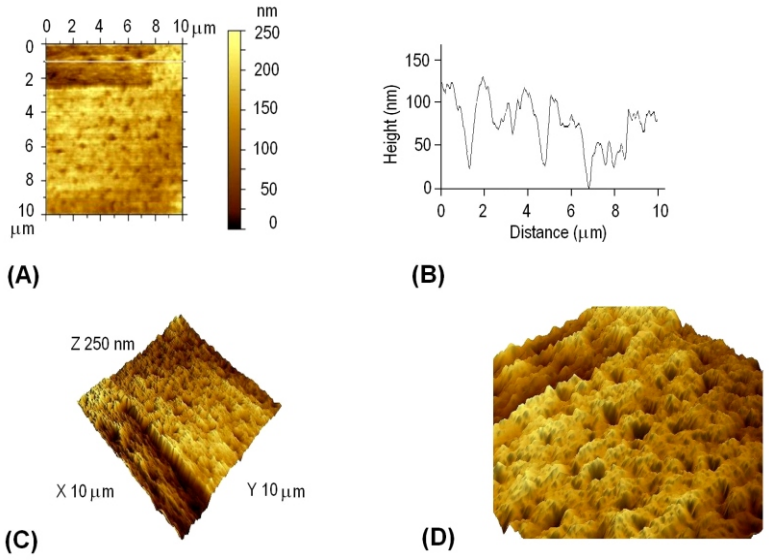

Fig. 7. AFM image of the DMPC-calixarene layer at the mica surface of the area 10 10 m^2: (A) 2D scan; (B) profile of the thickness along the line drawn in the image; (C) 3D image. (D) zoom of 3D image showed at (C).

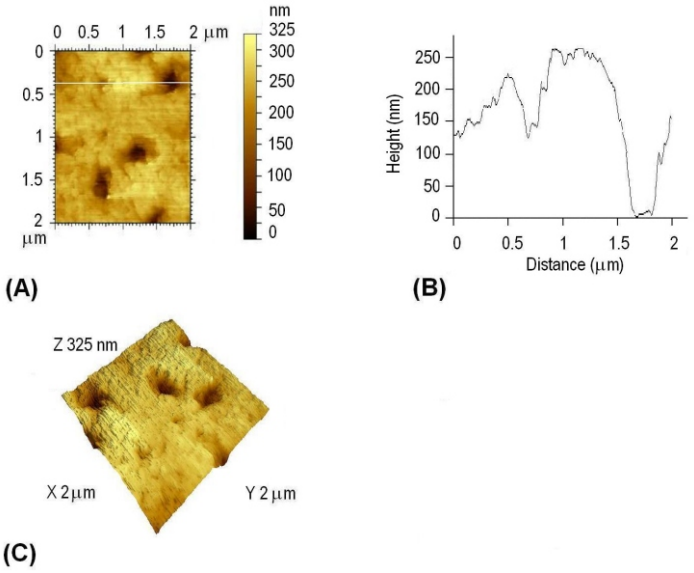

Fig. 8. AFM image of the DMPC-CX layer at the mica surface of the area 2 2 m^2: (A) 2D scan; (B) profile of the thickness along the line drawn in the image; (C) 3D image.

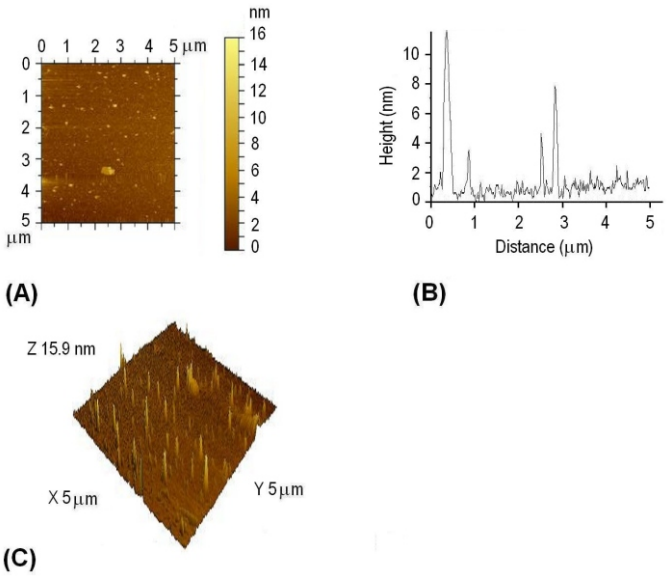

Fig. 9. AFM image of the DMPC-calixarene layer at the mica surface incubated with 30 nM cyt c. The scanned area: 5 5 m^2: (A) 2D scan; (B) profile of the thickness along the line drawn in the image; (C) 3D image.

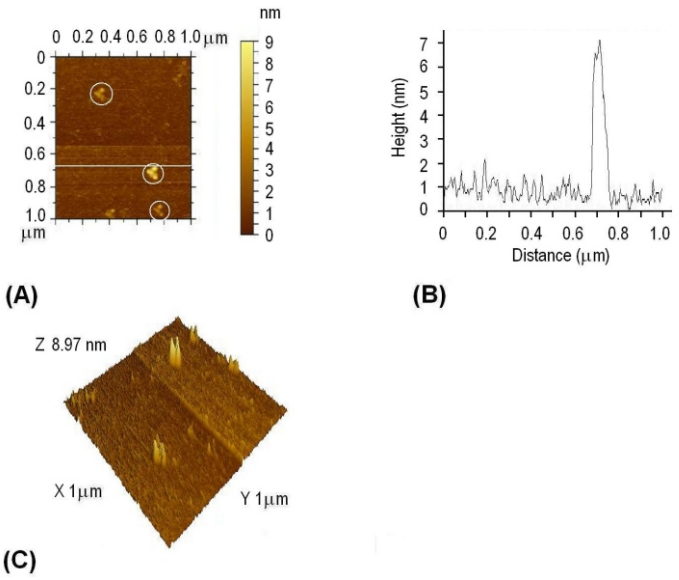

Fig. 10. AFM image of the DMPC-calixarene layer at the mica surface incubated with 30 nM cyt c. The scanned area: 1 1 m^2: (A) 2D scan; (B) profile of the thickness along the line drawn in the image. Aggregates of cyt c are marked by circles; (C) 3D image.

4. Conclusions

The dynamic light scattering method allowed us to study the effect of calixarenes (CX) on the size and zeta potential of large unilamellar vesicles of DMPC. We showed that with increased concentration of CX the size of LUV increases by 1.2 times. At the same time the zeta potential became more negative suggesting incorporation of CX into the outer monolayer of LUV and confirming the existence of negatively charged carboxyl groups in polar part of CX. At presence of cyt c (at concentrations above 10 M) the zeta potential is compensated due to positive charge of the protein. QCM method confirmed the specific interaction of cyt c with sBLM modified by CX. However, even at rather high concentration of cyt c we did not observe saturation of resonant frequency of quartz crystal transducer. This indicates formation of aggregates or fibers of cyt c. The AFM method allowed us to analyze topography of the mica surfaces covered by self-assembled layers of pure DMPC and that containing CX at presence of cyt c. The topography of DMPC layers agreed well with already published data and suggests ordered layers of rather small roughness. The roughness of the calixarene layer was about 5 times higher in comparison with that of DMPC, probably due to formation of monolayers and even multilayers of calixarenes. Novel and surprising result has been obtained for mixed DMPC-calixarene layers at presence of cyt c. Incubation of these layers with 30 nM of cyt c resulted in transformation of rather rough multilayers into the relatively flat layers containing sharp fibers of cyt c.

Acknowledgements

This work was financially supported by the Agency for Promotion Research and Development under the projects APVV-0362-07 and LPP-0250-09. This publication is also the result of the project implementation: "The centre of excellence for utilization of information on bio-macromolecules in disease prevention and in improvement of quality of life" (ITMS 26240120003) supported by the Research and Development Operational Programme funded by the ERDF. We thank to Dr. T. Oshima for generous gift of calixarene.

References

[1] T. Hianik: In: Bioelectrochemistry. Fundamentals, Experimental Techniques and Applications, P. N. Bartlett (Ed.); Wiley; Chichester; 2008, 87–156.
[2] D. P. Nikolelis, T. Hianik, G-P. Nikoleli: Electroanalysis **22** (2010) 2747–2763.
[3] R. Ludwig: Fresn. J. Anal. Chem. **367** (2000) 103–128.
[4] D. Gutsche: In: Calixarenes in the Nanoworld, J. Vicens, J. Harrowfield (Eds.), Springer, Dordrecht; 2007, 1–19.
[5] T. Oshima, H. Higuchi, K. Ohto, K. Inoue, M. Goto: Langmuir **21** (2005)7280–7284.
[6] Z. T.Schug, E. Gottlieb: Biochim. Biophys. Acta. **1788** (2009) 2022–2031.
[7] V. M. Trusova, G. P. Gorbenko, J. G. Molotkovsky, P. K. J. Kinnunen: Biophys. J. **99** (2010) 1754–1763.
[8] P. Vitovič, V. Šubjaková, T. Hianik, Thin Solid Films, submitted.
[9] M. A. Mohsin, F-G. Banica, T. Oshima, T. Hianik, Electroanalysis, 2011, in press.
[10] K. Ohto, M. Yano, K. Inoue, T. Yamamoto, M. Goto, F. Nakashio , S. Shinkai, T. Nagasaski: Anal. Sci. **11** (1995) 893–902.
[11] R. C. MacDonald, R. I. MacDonald, B. P. M. Menco, K. Takeshita, N. K. Subbarao, L. Hu, Biochim. Biophys. Acta, **106**1 (1991) 297–303.
[12] V. M. Mirsky, M. Mass, C. Krause, O. S. Wolfbeis: Anal. Chem. **70** (1998) 3674–3678.

[13] T. Hianik, V. Ostatná, M. Sonlajtnerova, I. Grman: Bioelectrochemistry **70** (2007) 127–133.
[14] P. Skladal, J. Horacek: Anal. Lett. **32** (1999) 1519–1529.
[15] D. Sarid: Exploring Scanning Probe Microscopy with Mathematica. Wiley, Chichester, 1997.
[16] M. C. Petty: Langmuir-Blodgett Films. An Introduction, Cambridge University Press, New York, 1996.
[17] C. M. A. Brett, A. M. Oliveira-Brett: Electrochemistry. Principles, Methods, and Applications. Oxford Science Publications, Oxford, 1993.
[18] D. P. F. Hoatson, F. E. Fellman, F. B. Mackay, M. Bloom: Biochemistry **25** (1986) 3804–3812.
[19] G. Sauerbrey: Z. Phys. **155** (1959) 206–210.
[20] G. L. Hayward, G. Z. Chu: Anal. Chim. Acta **288** (1994) 179–185.
[21] K. K. Kanazava, J. G. Gordon: Anal. Chim. Acta **175** (1985) 99–105.
[22] X. C. Zhou, L. Q. Huang, S. F. Y. Li: Biosens. Bioelectr. **16** (2001) 85–95.
[23] M. Snejdárkova, L. Svobodova, V. Polohova, T. Hianik: Anal. Bioanal. Chem. **390** (2008) 1087–1091.
[24] M. C. Phillips, E. A. Hauser: J. Coll. Interface Sci. **49** (1974) 31–39.
[25] S. J. Johnson, T. M. Bazeri, D. C. McDermott, G. W. Adam, A. R. Rennie, R. K. Thomas, E. Sackmann: Eur. Biophys. J. **59** (1991) 289-294.
[26] K. El Kirat, S. Morandat: Chem. Phys. Lipids **162** (2009) 17–24.
[27] J-M. Alakoskela, A. Jutila, A. C. Simonsen, J. Pirneskoski, S. Pyhajoki, R. Turunen, S. Marttila, O. G. Mouritsen, E. Goormaghtigh, P. K. J. Kinnunen: Biochemistry **45** (2006) 13447–13453.